

Light-Controlled Macrocyclization of Tetrathiafulvalene with Azobenzene: Designing an Optoelectronic Molecular Switch

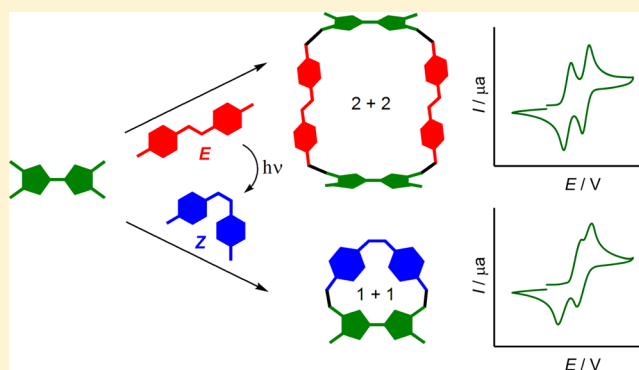
Vladimir A. Azov,^{*,†} Jens Cordes,[†] Dirk Schlüter,[†] Thomas Dülcks,[†] Marcus Böckmann,^{*,‡} and Nikos L. Doltsinis[‡]

[†]Department of Chemistry, University of Bremen, Leobener Strasse NW 2C, D-28359 Bremen, Germany

[‡]Institut für Festkörperttheorie and Center for Multiscale Theory & Computation, Westfälische Wilhelms-Universität Münster, Wilhelm-Klemm-Strasse 10, 48149 Münster, Germany

S Supporting Information

ABSTRACT: Macrocyclization between tetrathiafulvalene (TTF) dithiolates and bis-bromomethylazobenzenes/bis-bromomethylstilbenes is investigated under high dilution conditions. We show that macrocycles of different size can be formed depending on whether the (*Z*)- or (*E*)-isomers of azobenzene (AB) or stilbene are used. This represents the first example of a light-controllable cyclization reaction. The oxidation potential of the small, structurally rigid TTF–AB macrocycle is found to depend on the conformation of the AB moiety, opening the way for the modulation of redox properties by an optical stimulus. DFT calculations show that the out-of-plane distortion of the TTF moiety in this macrocycle is responsible for the variation of its oxidation potential upon photoisomerization of the neighboring AB bridge.



■ INTRODUCTION

Reversible light-induced *Z*–*E* isomerization of double bonds plays a central role in visual perception. Upon absorption of a photon by a photoreceptor cell in the eye retina, one of the double bonds of the chromophore 11-(*Z*) retinal isomerizes into the (*E*) configuration.^{1,2} This isomerization triggers the visual phototransduction cascades, in which photon energy is transformed into electric signal, which in turn is transmitted by neurons to the brain visual cortex, while *all-trans* retinal is converted in a multistep process back to 11-(*Z*) retinal. Thus, our visual perception is based on the transformation of a photon into an electrical signal via reversible isomerization of a photochromic molecule. To replicate this process in an artificial laboratory system remains a big challenge, which, if solved, could pave the way for a number of exciting technological applications.

As a possible design for a simple molecular system capable of altering its electronic properties when exposed to light, we have considered molecular architectures containing tightly connected photochromic and redox active units. We have selected azobenzenes³ (AB), which represent versatile and easily tunable photoswitches,⁴ as optical modulators for our systems. ABs can exist in two selectively accessible configurations, (*E*) and (*Z*), with pronounced geometrical and photophysical properties and, therefore, can significantly alter the conformation of molecular moieties tightly appended to them. Azobenzenes have been extensively employed for photomodulation of various properties, such as control of conformational changes and molecular

motion⁵ and of self-assembly processes⁶ on molecular and supramolecular levels and in biological systems.⁷

To induce the modulation of electronic properties, the AB moiety needs to be connected to a redox-active moiety that changes its electrochemical behavior upon its mechanical distortion. Therefore, we turned our attention to tetrathiafulvalenes⁸ (TTF), redox-active heterocyclic compounds displaying two consecutive reversible oxidation potentials, as possible electroresponsive units for our systems. TTFs are widely used in the field of organic electronics⁹ as well as redox-switching units¹⁰ in different types of molecular architectures,¹¹ such as interlocked supramolecular devices¹² or molecular receptors.^{13,14} It has been shown previously that the out-of-plane distortion of the tetrathiafulvalene backbone by linking its opposite ends using short molecular bridges leads to strong changes in its redox properties¹⁵ due to the lack of conjugation in the nonplanar TTF skeleton. Surprisingly, only few examples of tetrathiafulvalene–azobenzene (TTF–AB) conjugates have been reported to date.¹⁶ Two recent studies^{16c,17} report on photochromic TTF derivatives, both displaying a rather subtle influence of chromophore isomerization on the redox properties of the TTF unit.

In our approach, we bind TTF and AB moieties employing two short bridges (Figure 1) obtaining the rigid macrocycle **1**, in which optical as well as electrochemical switching of both groups

Received: October 28, 2014

Published: November 5, 2014

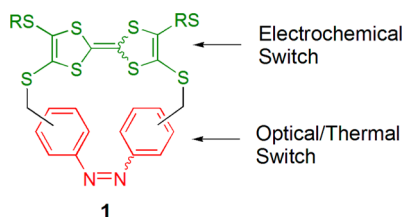


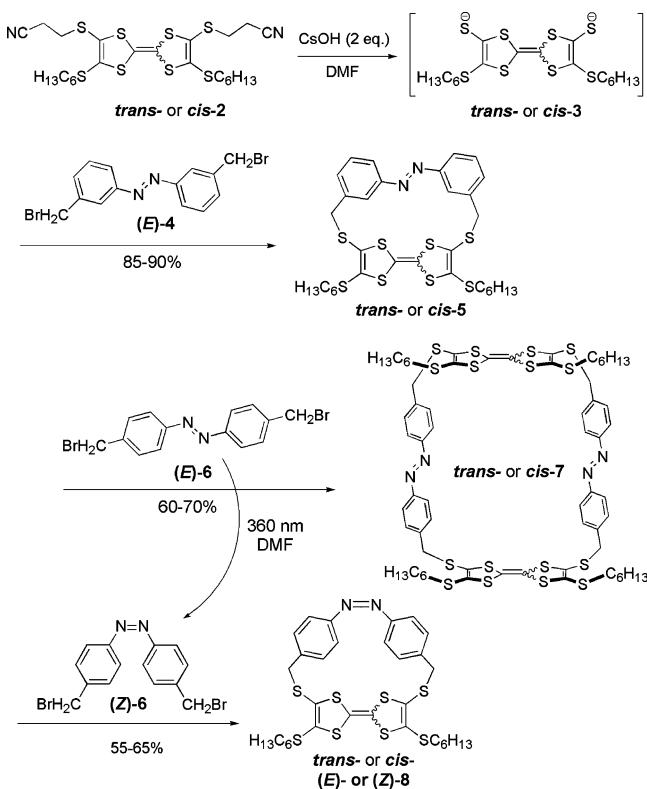
Figure 1. Concept of a multistate molecular device with orthogonal switching inputs.

are expected to display a significant influence on each other due to their tight mutual connection. Molecular modeling¹⁸ showed that tetrathio-substituted TTF and AB groups display a suitable size match with each other.

RESULTS AND DISCUSSION

For the macrocyclization reaction, *trans*- and *cis*-bis-cyanoethyl TTF derivatives¹⁹ *trans*-/*cis*-**2**²⁰ were taken and deprotected with the formation of dithiolates²¹ *trans*-/*cis*-**3**, which were allowed to react with the *m*-AB derivative²² (*E*)-**4** or the *p*-AB derivative (*E*)-**6** under high dilution conditions (Scheme 1). The

Scheme 1. Synthesis of Tetrathiafulvalene–Azobenzene Macrocycles



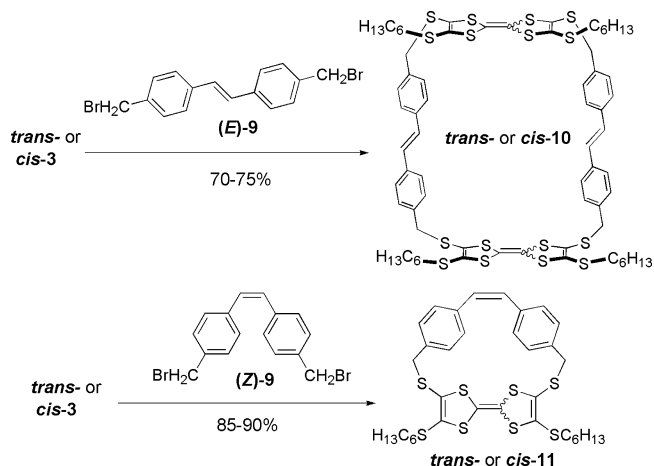
macrocyclization reaction afforded 1 + 1 cyclization products *trans*-/*cis*-**5** with *m*-AB (*E*)-**4** and 2 + 2 cyclization products *trans*-/*cis*-**7** with *p*-AB (*E*)-**6** with reasonably good yields. Although it was reported that large flexible TTF-containing macrocycles usually represent slowly interconverting inseparable *trans*/*cis*-TTF isomer mixtures,^{23,19a} the smaller *trans*-/*cis*-**5** macrocycles could be isolated and kept for prolonged time periods without significant isomerization of the TTF moiety. The larger macrocycles *trans*-/*cis*-**7** could be separated initially in almost pure form but tend to isomerize much faster than *trans*-/

cis-**5**. No higher molecular weight macrocycles or oligomers could be detected in the reaction mixture.²⁴

The results of the macrocyclization using the “longer” AB (*E*)-**6** imply that the size mismatch between dithiolates *trans*-/*cis*-**3** and (*E*)-**6** was the plausible cause for the inability to form smaller macrocycles. Upon isomerization from (*E*)-**6** to (*Z*)-**6** the distance between two terminal $-\text{CH}_2-$ groups shortens from ca. 12.1 Å to ca. 8.6 Å, making it comparable with the one in (*E*)-**4**, which is about 9.2–10.8 Å depending on its conformation and thus close to the distance between the S atoms of dithiolate, which is 9.3 Å for *cis*- and 9.9 Å for *trans*-dithiolate.¹⁸ In a macrocyclization reaction using **6** in a photostationary state with ca. 85:15 (*Z*)-**6**/*(E)*-**6** ratio (prepared by irradiation of (*E*)-**6** in DMF solution at 0 °C at 360 nm before the reaction), predominant formation of the 1 + 1 cyclization product **8** was obtained, whereas the 2 + 2 products were also detected in fairly small amounts (5–10%) using ESI-MS.²⁵ To our knowledge, this is the first example of macrocyclization control, which is achieved by selective photochemical isomerization of one of the building blocks immediately before the reaction.²⁶

Because of the configurational lability of the azobenzene bridge, it was impossible to establish if 2 + 2 cyclization products form due to the presence of residual (*E*)-**6** in the starting mixture or in the direct cyclization between dithiolates **3** and (*Z*)-**6**. Similar macrocyclizations using configurationally stable stilbene derivative²⁷ (*E*)-**9** afforded the formation of 2 + 2 products *trans*-/*cis*-**10**, whereas (*Z*)-**9** gave exclusively 1 + 1 products *trans*-/*cis*-**11** (Scheme 2), proving that the close AB–dithiolate

Scheme 2. Synthesis of Tetrathiafulvalene–Stilbene Macrocycles



size match is a prerequisite for a successful 1 + 1 macrocyclization. Both *trans*-/*cis*-**10** and *trans*-/*cis*-**11** could be separated and characterized as almost pure *trans*- or *cis*-isomers.

¹H NMR spectra of *trans*-/*cis*-**11** afforded invaluable information for the assignment of ¹H NMR spectra of the four slowly interconverting (Figure 2) isomers of **8**, which could be separated from each other using flash chromatography and were sufficiently stable for NMR characterization. Thus, ¹H NMR spectra of *trans*-/*cis*-**11** display very good correlation with the spectra of *trans*-/*cis*-(*Z*)-**8**, respectively, allowing the assignment of two (*Z*)-isomers in the ¹H NMR spectra of **8** (Figure 3). Two *trans*-/*cis*-(*E*)-**8** isomers were assigned on the basis of the multiplicity of the $-\text{CH}_2-$ signals adjacent to the AB bridges²⁸ as

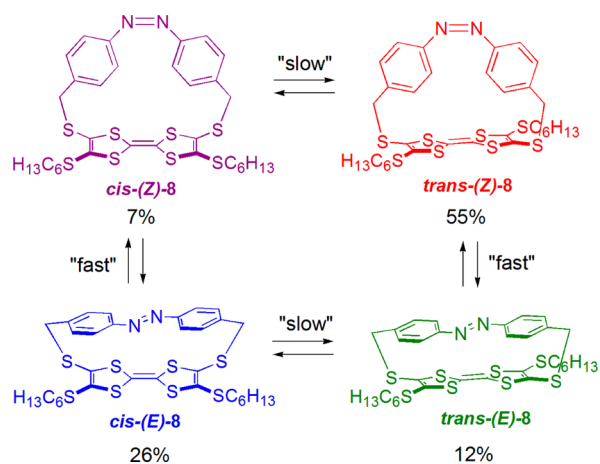


Figure 2. Conformer interconversion of four different isomers of **8**. Relative content of each isomer after the mixture was kept at 40 °C in CDCl₃ solution for a prolonged period of time are shown as mol % values below each isomer.

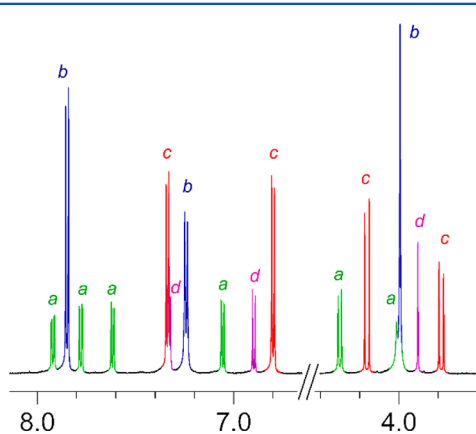


Figure 3. Cutouts of ¹H NMR spectra of the *trans*-/*cis*-(E/Z)-8 isomer mixture containing 26% of *trans*-(E)-8 (a, green), 37% of *cis*-(E)-8 (b, blue), 28% of *trans*-(Z)-8 (c, red), and 9% of *cis*-(Z)-8 (d, violet) isomers. Spectra of individual isomers in pure form are presented in the Supporting Information.

well as the multiplicity of the AB resonances in the aromatic region.²⁹

Due to impaired rotation of the TTF moiety in two *trans*-isomers of **8**, as well as in *trans*-**5** and *trans*-**11**, it imposes planar chirality to these macrocycle systems,³⁰ whereas 4,4'-substituted AB moiety can, in principle, serve as the second element of the planar chirality. Still, no formation of diastereomeric pairs for *trans*-(E)-**8** could be detected, which can be explained by the observation that the azo N=N moiety in ABs is rotating very rapidly in macrocycles³¹ and even in some crystal structures.³² Fixed asymmetric disposition of aromatic rings in *trans*-(E)-**8** manifests itself in the ¹H NMR spectrum (Figure 3): it is the only isomer of **8** displaying four multiplets in the aromatic region.

TTF-AB and TTF-stilbene macrocycles were obtained as bright yellow or yellow-orange stable crystalline powders. The smaller macrocycles **5**, **8**, and **11** display very good solubility in nonpolar organic solvents, such as CH₂Cl₂, toluene, or even alkenes. The larger macrocycles **7** and **10** are much less soluble and slowly precipitate even from CH₂Cl₂ or CHCl₃ solutions upon standing. Such poor solubility, which is more pronounced for the *cis*-isomers, can be explained by π -stacking interactions,

which should be much more favorable for the larger macrocycles capable of adopting almost planar conformations.

Heating of NMR samples in CDCl₃ of each of the four isomers of *trans*-/*cis*-(Z)-**8** to 40 °C in the dark led to the formation of similar isomer mixtures in ca. 3 weeks (Figure 2), indicating that the isomer *cis*-(Z)-**8** is the most thermodynamically stable one. To our knowledge, there are only very few examples of macrocyclic azobenzene derivatives, which favor the (Z)-isomer over the corresponding (E)-isomer.^{33–35} Relative energies of the different isomers obtained from DFT calculations (Table 1)

Table 1. Experimental Abundances and Theoretical Relative Energies (PBE0/6-31G*/PCM) of the Four Isomers of **8**

isomer	exp abundance (%)	theor rel energy (eV)
<i>trans</i> -(Z)- 8	55	0.00
<i>cis</i> -(E)- 8	26	0.10
<i>trans</i> -(E)- 8	12	0.16
<i>cis</i> -(Z)- 8	7	0.20

correspond well with experimentally observed abundances (Figure 2). Z-E interconversion of the AB moiety is relatively fast with a half-life of ca. 20 h at room temperature.³⁶ On the other hand, *cis*-*trans* isomerization of TTF is much slower with a half-life of several days at 40 °C in chloroform solution in the dark and most likely is induced by the trace amounts of acid present in the solution.³⁷ Similar isomerization studies using *trans*-(E)-**8** isomer as a starting material were performed in DMSO-*d*₆ and cyclohexane-*d*₁₂. The equilibrium ratio between *cis*-(E)-**8** and *cis*-(Z)-**8** isomers was 11:89 in DMSO-*d*₆ and 51:49 in cyclohexane-*d*₁₂, respectively, giving evidence for better stabilization of the more polar (Z)-isomer by polar media. No *trans* → *cis* isomerization of the TTF moiety was observed in DMSO-*d*₆ and in cyclohexane-*d*₁₂.

Optimized molecular structures of (Z)-isomers of **8** exhibit a distorted boat-shaped TTF, whereas in (E)-isomers the TTF moiety is fully planar being stretched by an oversized (E)-AB bridge (Figure 4). Two (Z)-isomers accommodate the AB unit in

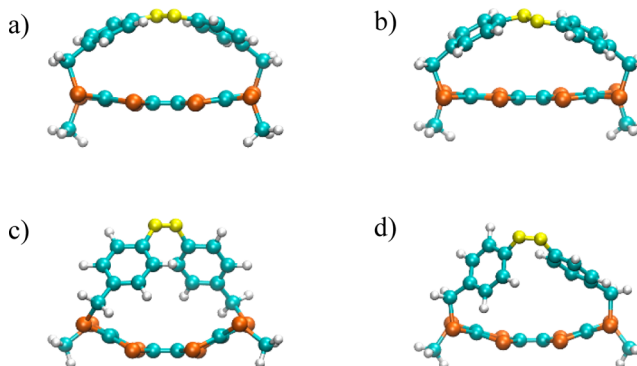


Figure 4. Optimized molecular structures of the four isomers of **8**: (a) *trans*-(E)-**8**, (b) *cis*-(E)-**8**, (c) *trans*-(Z)-**8**, (d) *cis*-(Z)-**8**.

a geometry close to that of the isolated molecule, while in the (E)-isomers it is bent with the C-N=N-C fragment displaying a deviation from planarity of about 20°. The molecular geometry of the isomers of **8** prohibits strong orbital interactions between the π -systems of the TTF and the AB moieties as the HOMOs are localized almost exclusively on the TTF units, whereas the LUMOs reside on the AB groups.

The UV/vis spectra (CH_2Cl_2 , 293 K) of the larger macrocycles show almost linear combinations of the absorption patterns of thioalkyl-substituted TTF derivatives with the absorption patterns of azobenzene, whereas smaller macrocycles **5** and **11** display more complex absorption patterns. UV/vis spectra of the four isomers of **8** can be separated into two groups with similar spectral properties, one comprising two (*E*)-isomers of *trans*-/*cis*-(*E*)-**8** and the other two (*Z*)-isomers *trans*-/*cis*-(*Z*)-**8** (Figure 5). Both (*E*)-isomers show absorption bands at ca. 350–370 nm, typical for (*E*)-AB, in experimental and modeled spectra.

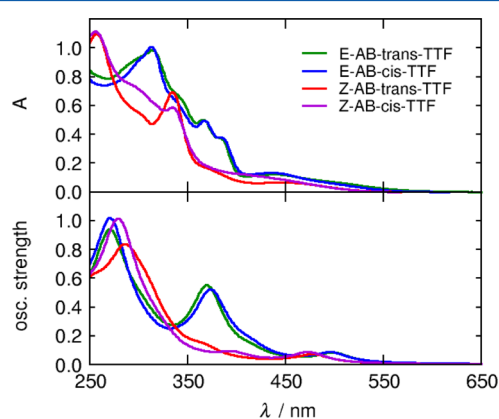


Figure 5. Experimental (above) and theoretical PBE0/6-31G*/PCM (below) UV/vis spectra of four isomers of **8** in CH_2Cl_2 : *trans*-(*E*)-**8** (green), *cis*-(*E*)-**8** (blue), *trans*-(*Z*)-**8** (red), and *cis*-(*Z*)-**8** (violet).

The larger nonstrained bis-TTF macrocycles **7** and **10** display the classical electrochemical behavior of TTF derivatives,^{9c} showing two reversible electrochemical processes on the cathodic scan, the first one leading to the double TTF^{•+} radical cation and the second affording the double dication TTF²⁺ (Figure 5 and Table 2) at the potentials common to tetrathiasubstituted TTFs.⁹ Much more interesting were the

Table 2. Electrochemical Data of the TTF–AB and TTF–Stilbene Macrocycles^a (Values in Parentheses Have Been Obtained from PBE0/6-31G*/PCM Calculations)^b

compound	$E_{1/2}^{\text{ox1}}$ (V)	$E_{1/2}^{\text{ox2}}$ (V)
large macrocycles:		
<i>trans</i> - 7	0.55	0.82
<i>cis</i> - 7	0.56	0.83
<i>trans</i> - 10	0.53	0.77
<i>cis</i> - 10	0.53	0.77
small macrocycles:		
<i>trans</i> - 5	0.62	0.91
<i>cis</i> - 5	0.62	0.91
<i>trans</i> -(<i>E</i>)- 8	0.46 (0.17)	0.90 (1.30)
<i>cis</i> -(<i>E</i>)- 8	0.46 (0.19)	0.90 (1.40)
<i>trans</i> -(<i>Z</i>)- 8	0.59 (0.42)	0.81 (1.33)
<i>cis</i> -(<i>Z</i>)- 8	0.59 (0.42)	0.80 (1.22)
<i>trans</i> - 11	0.58	0.79
<i>cis</i> - 11	0.58	0.78

^aData were obtained using a one-compartment cell in $\text{CH}_2\text{Cl}_2/0.1$ M Bu_4NClO_4 , Pt as the working and counter electrodes and a nonaqueous Ag/Ag⁺ reference electrode; scan rate 100 mV/s. Values given at room temperature vs SCE; the Fc/Fc⁺ couple (0.480 V vs SCE) was used as a potential reference.⁴⁰ ^bDetermined as described in ref 41, see the Supporting Information for details.

redox properties of the smaller TTF–AB macrocycles **5**, **8**, and **11**. Macrocycles *trans*-/*cis*-**5** displayed the expected “normal” CVs with both oxidation potentials lying slightly higher than the corresponding potentials of the 2 + 2 macrocycles. Both (*E*)-AB macrocycles *trans*-/*cis*-(*E*)-**8** also showed CVs common to TTF derivatives, although in their case the first oxidation potentials were significantly lower than those of the other macrocycles discussed above. On the other hand, the smaller macrocycles containing (*Z*)-AB or (*Z*)-stilbene showed a strong positive shift of the cathodic wave affording characteristic CVs very different from those of other TTF-containing macrocycles (Figure 6).

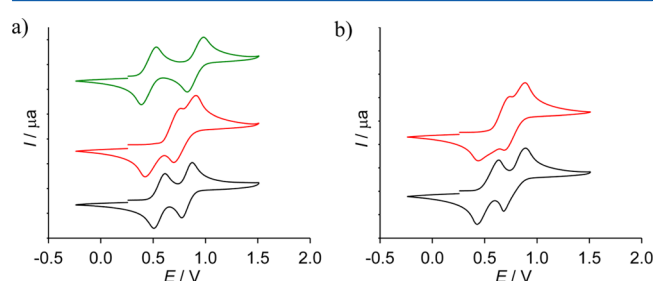


Figure 6. (a) Representative cyclic voltammograms of TTF–AB macrocycles *trans*-(*E*)-**8** (green), *trans*-(*Z*)-**8** (red), and *trans*-**7** (black) and (b) the corresponding TTF–stilbene macrocycles *trans*-**11** (red) and *trans*-**10** (black). $\text{CH}_2\text{Cl}_2/0.1$ M Bu_4NClO_4 , scan rate 100 mV/s, potentials plotted vs SCE.

Thus, electrochemical properties of a TTF moiety are strongly dependent on the macrocycle size as well as on the configuration of an AB or stilbene moiety,³⁸ whereas its own configuration does not display any significant influence.³⁹ We also need to note that azobenzenes and stilbenes do not display any redox activity in the scan range used for the macrocycle characterization and all redox processes are centered on the TTF moieties.

DFT calculations for the different isomers of **8** in their neutral and cationic states¹⁸ displayed good agreement with the experiment: the first oxidation potentials of (*Z*)-AB-isomers are higher than those of (*E*)-AB-isomers, while *cis*–*trans* isomerization of TTF has a negligible effect. The theoretical differences of 0.25 and 0.23 eV for *trans*-*E*/*Z* and *cis*-*E*/*Z*, respectively, are only slightly larger than the corresponding experimental difference of 0.13 eV. The absolute theoretical first oxidation potentials are consistently smaller than the experimental ones by 0.2 eV on average, since they are estimated using an empirical correction coefficient.⁴¹ Theory also correctly predicts the opposite trend for the second oxidation potential: averaged over *cis*- and *trans*-isomers, it is 0.07 eV lower for the *E* species than for the *Z* species, thus matching well the experimental *E*/*Z* difference of 0.09 eV. Additionally, the difference of the second oxidation potential between the *E* and *Z* isomers is less pronounced than for the first oxidation potential.

Preliminary UV/vis irradiation experiments of one of the isomers of **8** using different wavelengths and followed by UV/vis spectroscopy have shown that the conformational states of **8** can be successfully controlled by external light irradiation.¹⁸ The influence of chemical modification, mechanical constraints, and the molecular environment on the mechanism and efficiency of AB photoisomerization has been the subject of numerous recent investigations.^{33a,42,43} It is now accepted knowledge that photoisomerization of AB in the S_1 excited state proceeds by a space-conserving pedal-like twisting motion of the N=N double

bond and, thus, can be efficiently invoked even in mechanically constrained systems such as the one proposed here. Orbital analysis¹⁸ gives evidence that transitions, localized on AB moieties, can be excited separately by irradiation at a specific wavelength. Chemical modifications of the AB moiety, such as fluorination, should allow shifting of $n \rightarrow \pi^*$ transitions of the (*E*)- and (*Z*)-isomers in a visible region,⁴⁴ affording better separation from the absorption bands of the TTF group. Moreover, 5,6-dihydrodibenzo[*c,g*][1,2]diazocine³³ can be suggested as an optional photochemical switching unit with distinguished geometrical differences between the two accessible configurations.

CONCLUSIONS

To conclude, we have shown the first example of photochemically controlled macrocyclization, in which the formation of smaller 1 + 1 and larger 2 + 2 cyclization products can be modulated by photoisomerization of one of the components before the reaction. Its product, azobenzene-containing macrocycle **8**, is one of the rare azobenzene derivatives with a thermodynamically more stable (*Z*)-isomer. We have achieved separation of four isomers of **8** and have shown that the electrochemical properties of the tetrathiafulvalene unit are strongly influenced by the configuration of the azobenzene moiety. DFT calculations were employed to rationalize the observed behavior of macrocycle **8**. Detailed photophysical and spectroelectrochemical studies of the new TTF–AB derivatives should be reported in the due course.

EXPERIMENTAL SECTION

Materials and Methods. Tetrathiafulvalene derivatives *trans*-/*cis*-2,¹⁹ azobenzene derivatives (*E*)-**4** and (*E*)-**6**,²² and stilbene derivatives (*E*/*Z*)-**9**²⁷ were prepared as described previously. Reagent-grade chemicals and solvents were used without further purification unless otherwise stated. All reactions were carried out under an atmosphere of dry N₂. NMR chemical shifts (δ) are reported in parts per million (ppm) downfield from tetramethylsilane, and residual solvent signals (7.26 ppm for ¹H, 77.0 ppm for ¹³C in CDCl₃, 5.32 ppm for ¹H, 53.8 ppm for ¹³C in CD₂Cl₂) were used as references. ¹H NMR coupling constants (*J*) are reported in hertz (Hz), and multiplicity is indicated as follows: s (singlet), d (doublet), t (triplet), q (quintet). High-resolution ESI-MS spectra (HRMS) were measured on an LTQ Orbitrap spectrometer. Observed isotopic patterns of the [M]⁺ and [M]²⁺ ions of all new compounds were fully consistent with the calculated ones. UV/vis measurements were performed in a 1 cm path length quartz optical cell. Melting points were determined using a capillary melting point apparatus and are uncorrected. *R_f* values were determined using 0.2 mm silica gel F-254 TLC cards. Flash chromatography (FC) was carried out using 230–440 mesh (particle size 36–70 μ m) silica gel. Photoisomerization of azobenzene was carried out in a custom-built photoreactor with two 25 W “blacklight” low pressure mercury lamps. Cyclic voltammetry (CV) measurements were performed in a three-electrode single-compartment cell.¹⁸

Macrocyclization Reaction, General Procedure. Bis-cyanoethyl TTF derivative **2** was dissolved in dry DMF, degassed by two freeze–pump–thaw cycles and cooled to 0 °C, and then CsOH (1.46 M solution in MeOH) was added within 10 min. The mixture was allowed to warm to rt being stirred for 1 h, changing its color from orange to dark brown-red upon buildup of TTF-dithiolate **3**. Then a solution of dibromoazobenzene derivative **4/6** or dibromostilbene derivative **9** in dry degassed DMF was added in one portion to the dithiolate solution at 0 °C, and the reaction mixture was stirred overnight. Reactions with azobenzene (*Z*)-**6** were performed in flasks wrapped with aluminum foil to maintain the light isolation. The color of the reaction gradually turned orange-yellow, and an orange or yellow precipitate could form for some derivatives. Then DMF was removed under vacuum at 30–40 °C using

Kugelrohr distillation, and the crude product was purified using flash chromatography (FC) on SiO₂.

***E* → *Z* Isomerization of (1*E*)-1,2-Bis[3-(bromomethyl)phenyl]diazene (*E*)-**9**.** Isomerization time was first optimized by irradiation of 1.6 mg azobenzene (*E*)-**9** in 0.65 mL of DMF-*d*₇ upon stirring at 0 °C and controlling the reaction using ¹H NMR at 30 min intervals.

(*E*)-**9**: ¹H NMR (200 MHz, DMF-*d*₇) 4.56 (s, 4H), 7.53–7.57 (m, 4H), 7.88–7.92 (m, 4H).

(*Z*)-**9**: ¹H NMR (200 MHz, DMF-*d*₇) 4.42 (s, 4H), 6.81–6.85 (m, 4H), 7.27–7.31 (m, 4H).

NMR experiments have shown that the photostationary state with ca. 85% of (*Z*)-**9** is reached within 1–1.5 h. Additionally, an (*E*/*Z*)-**9** mixture can be analyzed using UV–vis and TLC, but only qualitative assessment is possible using these methods.

For the preparative isomerization, azobenzene (*E*)-**9** was dissolved in dry DMF, degassed by two freeze–pump–thaw cycles, cooled to 0 °C, and irradiated with two 25 W “blacklight” low-pressure mercury lamps for 2 h upon stirring. Then it was taken into a heat- and light-isolated syringe and added to the dithiolate solution.

Macrocycle *trans*-5. Prepared from *trans*-**2** (0.056 g, 0.092 mmol) and CsOH (1.46 M, 0.125 mL, 0.183 mmol) in 15 mL of DMF upon addition of azobenzene (*E*)-**4** (0.033 g, 0.89 mmol) in 15 mL of DMF. The product was purified by FC (CH₂Cl₂/cyclohexane, 1:1) to afford an orange crystalline powder. Yield: 0.059 g (0.084 mmol, 94%). Mp: 79–82 °C. *R_f* = 0.65 (CH₂Cl₂/cyclohexane, 1:1). ¹H NMR (200 MHz, CDCl₃): δ 0.72 (t, ³*J* = 6.7 Hz, 6H), 0.91–1.20 (m, 16H), 2.16–2.48 (m, 4H), 3.76 (d, ²*J* = 13.5 Hz, 2H), 4.33 (d, ²*J* = 13.5 Hz, 2H), 7.43–7.53 (m, 6H), 7.67–7.72 (m, 2H). ¹³C NMR (50 MHz, CDCl₃): δ 13.9, 22.4, 27.9, 29.0, 30.9, 36.2, 39.7, 114.2, 121.1, 123.4, 124.9, 129.4, 130.8, 134.5, 138.8, 152.6. UV/vis (CH₂Cl₂): λ_{\max} (ϵ) 304 nm (24500 L·mol⁻¹·cm⁻¹), 327 (26000). MS (ESI⁺): *m/z* 706 [M]⁺, 729 [M + Na]⁺, 745 [M + K]⁺. MS (ESI⁻): *m/z* 705 [M – H]⁻. HRMS (ESI⁺): *m/z* [M]⁺ calcd for C₃₂H₃₈N₂S₈⁺ 706.07952, found 706.08026. CV (vs SCE, CH₂Cl₂): *E*_{1/2}^{ox1} = 0.62 V, *E*_{1/2}^{ox2} = 0.91 V.

Macrocycle *cis*-5. Prepared from *cis*-**2** (0.097 g, 0.159 mmol) and CsOH (1.46 M, 0.22 mL, 0.321 mmol) in 30 mL of DMF upon addition of azobenzene (*Z*)-**4** (0.059 g, 0.159 mmol) in 30 mL of DMF. The product was purified by FC (CH₂Cl₂/cyclohexane, 1:1) to afford red-brown crystalline powder. Yield: 0.101 g (0.143 mmol, 90%). Mp: 155–156 °C. *R_f* = 0.58 (CH₂Cl₂/cyclohexane, 1:1). ¹H NMR (200 MHz, CDCl₃): δ 0.88 (t, ³*J* = 6.5 Hz, 6H), 1.19–1.36 (m, 16H), 2.39 (t, ³*J* = 6.9 Hz, 4H), 4.05 (s, 4H), 7.38–7.48 (m, 4H), 7.73–7.83 (m, 2H), 8.03–8.05 (m, 2H). ¹³C NMR (50 MHz, CDCl₃): δ 14.0, 22.4, 28.1, 29.1, 31.1, 36.2, 39.2, 109.9, 120.5, 122.1, 126.3, 129.2, 131.2, 135.9, 137.3, 151.5. UV/vis (CH₂Cl₂): λ_{\max} (ϵ) 309 nm (28000 L·mol⁻¹·cm⁻¹), 327 (27300). MS (ESI⁺): *m/z* 706 [M]⁺, 729 [M + Na]⁺, 745 [M + K]⁺; MS (ESI⁻): *m/z* 705 [M – H]⁻. HRMS (ESI⁺): *m/z* [M]⁺ calcd for C₃₂H₃₈N₂S₈⁺ 706.07952, found 706.08000. CV (vs SCE, CH₂Cl₂): *E*_{1/2}^{ox1} = 0.62 V, *E*_{1/2}^{ox2} = 0.91 V.

Macrocycle *trans*-7. Prepared from *trans*-**2** (0.040 g, 0.066 mmol) and CsOH (1.46 M, 0.091 mL, 0.133 mmol) in 15 mL of DMF upon addition of azobenzene (*E*)-**6** (0.024 g, 0.066 mmol) in 10 mL of DMF. The product was purified by FC (CH₂Cl₂/cyclohexane, 1:1) to afford an orange crystalline powder. The fresh product showed only one spot on TLC plates, and two minor spots with lower *R_f* values slowly appeared after keeping the substance at rt in a solution. Yield: 0.031 g (0.022 mmol, 66%). Mp: 175–180 °C dec. *R_f* = 0.57 (CH₂Cl₂/cyclohexane, 1:1). ¹H NMR (200 MHz, CDCl₃): δ 0.74–0.81 (m, 12H), 1.16–1.38 (m, 32H), 2.50 (t, ³*J* = 7.3 Hz, 8H), 3.97 (s, 8H), 7.38–7.42 (m, 8H), 7.87–7.91 (m, 8H). ¹³C NMR (50 MHz, CDCl₃): δ 13.9, 22.4, 28.1, 29.4, 31.1, 36.3, 40.0, 110.5, 122.9, 124.3, 129.7, 133.1, 140.7, 151.8. UV/vis (CH₂Cl₂): λ_{\max} (ϵ) 332 nm (78500 L·mol⁻¹·cm⁻¹). MS (ESI⁺): *m/z* 1412 [M]²⁺, 1435 [M + Na]⁺, 1451 [M + K]⁺, 706 [M]⁺. MS (ESI⁻): *m/z* 1411 [M – H]⁻. HRMS (ESI⁺): *m/z* [M]²⁺ calcd for C₆₄H₇₆N₄S₁₆²⁺ 1412.15958, found 1412.16056. CV (vs SCE, CH₂Cl₂): *E*_{1/2}^{ox1} = 0.55 V, *E*_{1/2}^{ox2} = 0.82 V.

Macrocycle *cis*-7. Prepared from *cis*-**2** (0.100 g, 0.165 mmol) and CsOH (1.46 M, 0.23 mL, 0.336 mmol) in 30 mL of DMF upon addition of azobenzene (*E*)-**6** (0.064 g, 0.173 mmol) in 30 mL of DMF. The product was purified by FC (CH₂Cl₂/cyclohexane, 1:1) to afford orange

crystalline powder. The fresh product showed only one spot on TLC plates, and two minor spots with higher R_f values slowly appeared after the substance was kept at rt in solution. Yield: 0.079 g (0.056 mmol, 68%). Mp: 200–210 °C dec. R_f = 0.45 (CH₂Cl₂/cyclohexane, 1:1). ¹H NMR (200 MHz, CDCl₃): δ 0.75–0.81 (m, 12H), 1.14–1.38 (m, 32H), 2.47 (t, ³J = 7.3 Hz, 8H), 4.01 (s, 8H), 7.37–7.41 (m, 8H), 7.83–7.87 (m, 8H). ¹³C NMR (50 MHz, CDCl₃): δ 14.0, 22.5, 28.2, 29.5, 31.2, 36.3, 40.0, 123.0, 123.1, 129.6, 129.7, 140.3, 140.7, 151.9. UV/vis (CH₂Cl₂): λ_{max} (ε) 332 nm (77500 L·mol⁻¹·cm⁻¹). MS (ESI⁺): m/z 1412 [M]⁺, 1435 [M + Na]⁺, 706 [M]²⁺. MS (ESI⁻): m/z 1411 [M - H]⁻. HRMS (ESI⁺): m/z [M]⁺ calcd for C₆₄H₇₆N₄S₁₆⁺ 1412.15958, found 1412.16034. CV (vs SCE, CH₂Cl₂): $E_{1/2}^{ox1}$ = 0.56 V, $E_{1/2}^{ox2}$ = 0.83 V.

Macrocycles *trans*-/*cis*-(*E*/*Z*)-8. Prepared from *trans*-2 (0.050 g, 0.082 mmol) and CsOH (1.46 M, 0.115 mL 0.168 mmol) in 10 mL of DMF upon addition of azobenzene (*Z*)-6 (0.030 g, 0.082 mmol) in 10 mL of DMF. After removal of DMF performed under oil pump vacuum at 20 °C, the residue was dissolved in ca. 2 mL of CH₂Cl₂/cyclohexane, (1:2), and poorly soluble [2 + 2]-cyclization byproducts were filtered off. The remaining isomer mixture was separated by FC (CH₂Cl₂/cyclohexane, gradient 1:2 → 2:1), and any extensive illumination of the column and collected fractions was avoided. First, nonpolar (*E*)-azobenzene derivatives *trans*-(*E*)-8 and *cis*-(*E*)-8 were eluted, quickly followed by traces of [2 + 2] macrocyclization products and other minor byproducts of unknown nature, whereas (*Z*)-azobenzene derivatives *trans*-(*Z*)-8 and *cis*-(*Z*)-8 were eluted at the end. Collected fractions were concentrated and dried in full darkness. All isomers were obtained as orange or dark orange crystalline powders. Melting points were not measured due to conformational lability of the products. Yields: *trans*-(*E*)-8 0.009 g (0.013 mmol, 15%); *cis*-(*E*)-8 0.0025 g (0.0035 mmol, 4%); *trans*-(*Z*)-8 0.025 g (0.035 mmol, 43%); *cis*-(*Z*)-8 0.006 g (0.0085 mmol, 10%). Total yield of *trans*-/*cis*-(*E*/*Z*)-8: 0.0425 g (0.060 mmol, 73%).

Alternatively, *trans*-/*cis*-(*E*/*Z*)-8 was prepared from *cis*-2 (0.050 g, 0.082 mmol) and CsOH (1.46 M, 0.115 mL 0.168 mmol) in 10 mL of DMF upon addition of azobenzene (*Z*)-6 (0.031 g, 0.084 mmol) in 10 mL of DMF. Workup and purification as above. Yields: *trans*-(*E*)-8 traces; *cis*-(*E*)-8 0.0055 g (0.0078 mmol, 9%); *trans*-(*Z*)-8 0.005 g (0.0071 mmol, 9%); *cis*-(*Z*)-8 0.0305 g (0.043 mmol, 52%). Total yield of *trans*-/*cis*-(*E*/*Z*)-8: 0.041 g (0.058 mmol, 71%).

To obtain high-purity products, after the first chromatographic separation all isomers were mixed together and allowed to stay at room temperature in CH₂Cl₂ solution for several days. It allowed all byproducts containing (*Z*)-azobenzene moiety to isomerize into (*E*)-isomers with higher R_f values and not to interfere with the separation of the polar (*Z*)-8 macrocycles. R_f values were also used as an additional proof for the assignment of the (*E*)- and (*Z*)-isomer pairs of four: *trans*-/*cis*-(*E*)-8 display much higher R_f values in comparison with *trans*-/*cis*-(*Z*)-8, which is in agreement with R_f values and relative polarities of parent (*E*)-/(*Z*)-azobenzenes.

***trans*-(*E*)-8.** R_f = 0.65 (CH₂Cl₂/cyclohexane, 1:1). R_f = 0.48 (CH₂Cl₂/cyclohexane, 1:2). ¹H NMR (360 MHz, CD₂Cl₂): δ 0.88 (t, ³J = 7.0 Hz, 6H), 1.21–1.43 (m, 16H), 1.59 (qint, ³J = 7.6 Hz, 4H), 2.71–2.87 (m, 4H), 4.00 (d, 2H), 4.30 (d, ²J = 10.8 Hz, 2H), 7.05 (dd, ³J₁ = 8.4 Hz, ⁴J₂ = 2.05 Hz, 2H), 7.61 (dd, ³J₁ = 8.2 Hz, ⁴J₂ = 2.05 Hz, 2H), 7.78 (dd, ³J₁ = 8.4 Hz, ⁴J₂ = 2.05 Hz, 2H), 7.92 (dd, ³J₁ = 8.2 Hz, ⁴J₂ = 2.05 Hz, 2H). ¹³C NMR (90 MHz, CD₂Cl₂): δ 14.1, 22.9, 28.5, 30.1, 31.6, 36.0, 40.4, 116.7, 122.7, 131.2, 131.5, 131.7, 136.7, 137.5, 153.9. UV/vis (CH₂Cl₂): λ_{max} 311 nm, 366, 380 sh, 438. CV (vs SCE, CH₂Cl₂): $E_{1/2}^{ox1}$ = 0.46 V, $E_{1/2}^{ox2}$ = 0.90 V.

***cis*-(*E*)-8.** R_f = 0.60 (CH₂Cl₂/cyclohexane, 1:1). R_f = 0.40 (CH₂Cl₂/cyclohexane, 1:2). ¹H NMR (360 MHz, CD₂Cl₂): δ 0.89 (t, ³J = 7.0 Hz, 6H), 1.26–1.45 (m, 16H), 1.64 (qint, ³J = 7.4 Hz, 4H), 2.86 (t, ³J = 7.4 Hz, 4H), 4.0 (s, 4H), 7.23–7.26 (m, 4H), 7.83–7.86 (m, 2H). ¹³C NMR (90 MHz, CD₂Cl₂): δ 14.1, 22.9, 28.5, 30.2, 31.6, 36.1, 40.7, 104.6, 122.6, 124.3, 130.8, 136.3, 139.3, 154.8. UV/vis (CH₂Cl₂): λ_{max} 311 nm, 366, 382 sh, 435. CV (vs SCE, CH₂Cl₂): $E_{1/2}^{ox1}$ = 0.46 V, $E_{1/2}^{ox2}$ = 0.90 V.

***trans*-(*Z*)-8.** R_f = 0.23 (CH₂Cl₂/cyclohexane, 1:1). R_f = 0.12 (CH₂Cl₂/cyclohexane, 1:2). ¹H NMR (360 MHz, CD₂Cl₂): δ 0.86 (t, ³J = 7.0 Hz, 6H), 1.21–1.45 (m, 16H), 2.46–2.59 (m, 4H), 3.78 (d, ²J =

14.0 Hz, 2H), 4.16 (d, ²J = 14.0 Hz, 2H), 6.78–6.82 (m, 4H), 7.32–7.36 (m, 4H). ¹³C NMR (90 MHz, CD₂Cl₂): δ 14.1, 22.9, 28.5, 29.5, 31.4, 37.6, 40.2, 117.2, 120.7, 125.7, 130.4, 131.4, 137.6, 150.8. UV/vis (CH₂Cl₂): λ_{max} 255 nm, 333, 445 sh. CV (vs SCE, CH₂Cl₂): $E_{1/2}^{ox1}$ = 0.59 V, $E_{1/2}^{ox2}$ = 0.81 V.

***cis*-(*Z*)-8.** R_f = 0.14 (CH₂Cl₂/cyclohexane, 1:1). R_f = 0.07 (CH₂Cl₂/cyclohexane, 1:2). ¹H NMR (360 MHz, CD₂Cl₂): δ 0.89 (t, ³J = 7.0 Hz, 6H), 1.26–1.45 (m, 16H), 1.62 (qint, ³J = 7.4 Hz, 4H), 2.82 (t, ³J = 7.4 Hz, 4H), 3.91 (s, 4H), 6.88–6.92 (m, 4H), 7.31–7.35 (m, 4H). ¹³C NMR (90 MHz, CD₂Cl₂): δ 14.1, 22.8, 28.4, 30.0, 31.5, 36.4, 39.5, 120.6, 130.3 (the list is incomplete since the chemical shifts were obtained from a DEPT-135 spectrum, direct ¹³C NMR measurement was not possible due to fast isomerization of the product). UV/vis (CH₂Cl₂): λ_{max} 254 nm, 332. CV (vs SCE, CH₂Cl₂): $E_{1/2}^{ox1}$ = 0.59 V, $E_{1/2}^{ox2}$ = 0.80 V.

MS (ESI⁺), isomer mixture: m/z 706 [M]⁺, 729 [M + Na]⁺, 745 [M + K]⁺. MS (ESI⁻): m/z 705 [M - H]⁻. HRMS (ESI⁺), isomer mixture: m/z [M]⁺ calcd for C₃₂H₃₈N₂S₈⁺ 706.07952, found 706.08020.

Macrocyclic *trans*-10. Prepared from *trans*-2 (0.176 g, 0.291 mmol) and CsOH (1.46 M, 0.584 mmol, 0.400 mL) in 40 mL of DMF upon addition of stilbene (*E*)-9 (0.107 g, 0.291 mmol) in 40 mL of DMF. The product was purified by FC (CH₂Cl₂/cyclohexane, 1:1) to afford orange crystalline powder. Yield: 0.148 g (0.105 mmol, 72%). Mp: 169–170 °C. R_f = 0.65 (CH₂Cl₂/cyclohexane, 1:1). ¹H NMR (200 MHz, CDCl₃): δ 0.80–0.86 (m, 12H), 1.17–1.46 (m, 32H), 2.56 (t, ³J = 7.2 Hz, 8H), 3.95 (s, 8H), 7.07 (s, 4H), 7.25–7.29 (m, 8H), 7.41–7.46 (m, 8H). ¹³C NMR (50 MHz, CDCl₃): δ 14.0, 22.5, 28.2, 29.5, 31.2, 36.2, 40.0, 110.0, 125.2, 126.5, 128.2, 129.2, 131.9, 136.3, 137.0. UV/vis (CH₂Cl₂): λ_{max} (ε) 322 nm (89000 L·mol⁻¹·cm⁻¹). MS (ESI⁺): m/z 1408 [M]⁺, 1431 [M + Na]⁺, 1447 [M + K]⁺, 705 [M]²⁺. MS (ESI⁻): m/z 1407 [M - H]⁻. HRMS (ESI⁺): m/z [M]⁺ calcd for C₆₈H₈₀S₁₆⁺ 1408.17859, found 1408.17987. CV (vs SCE, CH₂Cl₂): $E_{1/2}^{ox1}$ = 0.53 V, $E_{1/2}^{ox2}$ = 0.77 V.

Macrocyclic *cis*-10. Prepared from *cis*-2 (0.107 g, 0.177 mmol) and CsOH (1.46 M, 0.358 mmol, 0.245 mL) in 30 mL of DMF upon addition of stilbene (*E*)-9 (0.60 mg, 0.178 mmol) in 30 mL of DMF. The product was purified by FC (CH₂Cl₂/cyclohexane, 1:1) to afford orange crystalline powder. Yield: 0.095 g (67 mmol, 76%). Mp: 190–195 °C dec. R_f = 0.65 (CH₂Cl₂/cyclohexane, 1:1). ¹H NMR (200 MHz, CDCl₃): δ 0.79–0.86 (m, 12H), 1.21–1.45 (m, 32H), 2.54 (t, ³J = 7.2 Hz, 8H), 3.97 (s, 8H), 6.99 (s, 4H), 7.22–7.26 (m, 8H), 7.35–7.39 (m, 8H). ¹³C NMR (50 MHz, CDCl₃): δ 14.0, 22.5, 28.2, 29.4, 31.2, 36.3, 40.3, 111.0, 125.7, 126.5, 128.1, 129.2, 131.4, 136.3, 136.8. UV/vis (CH₂Cl₂): λ_{max} (ε) 322 nm (88000 L·mol⁻¹·cm⁻¹). MS (ESI⁺): m/z 1408 [M]⁺, 1431 [M + Na]⁺, 1447 [M + K]⁺, 705 [M]²⁺. MS (ESI⁻): m/z 1407 [M - H]⁻. HRMS (ESI⁺): m/z [M]⁺ calcd for C₆₈H₈₀S₁₆⁺ 1408.17859, found 1408.17930. CV (vs SCE, CH₂Cl₂): $E_{1/2}^{ox1}$ = 0.53 V, $E_{1/2}^{ox2}$ = 0.77 V.

Macrocyclic *trans*-11. Prepared from *trans*-2 (0.151 g, 0.249 mmol) and CsOH (1.46 M, 0.350 mL, 0.511 mmol) in 40 mL of DMF upon addition of stilbene (*Z*)-9 (0.091 g, 0.250 mmol) in 30 mL of DMF. The product was purified by FC (CH₂Cl₂/cyclohexane, 1:1) to afford bright yellow crystalline powder. Yield: 0.146 g (0.207 mmol, 83%). Mp: 106–108 °C. R_f = 0.73 (CH₂Cl₂/cyclohexane, 1:1). ¹H NMR (200 MHz, CDCl₃): δ 0.81–0.87 (m, 6H), 1.19–1.32 (m, 16H), 2.41–2.49 (m, 4H), 3.70 (d, ²J = 13.6 Hz, 2H), 4.20 (d, ²J = 13.6 Hz, 2H), 6.50 (s, 2H), 6.98–7.04 (m, 4H), 7.18–7.24 (m, 4H). ¹³C NMR (50 MHz, CDCl₃): δ 14.0, 22.6, 28.2, 29.0, 31.0, 37.3, 40.0, 117.2, 126.6, 128.6, 129.2, 129.7, 131.0, 135.9, 136.1. UV/vis (CH₂Cl₂): λ_{max} (ε) 264 nm (22900 L·mol⁻¹·cm⁻¹), 332 (17000). MS (ESI⁺): m/z 704 [M]⁺, 727 [M + Na]⁺, 743 [M + K]⁺. MS (ESI⁻): m/z 703 [M - H]⁻. HRMS (ESI⁺): m/z [M]⁺ calcd for C₃₄H₄₀S₈⁺ 704.08902, found 704.08968. CV (vs SCE, CH₂Cl₂): $E_{1/2}^{ox1}$ = 0.58 V, $E_{1/2}^{ox2}$ = 0.79 V.

Macrocyclic *cis*-11. Prepared from *cis*-2 (0.153 g, 0.253 mmol) and CsOH (1.46 M, 0.350 mL, 0.511 mmol) in 40 mL of DMF upon addition of stilbene (*Z*)-9 (0.091 g, 0.250 mmol) in 30 mL of DMF. The product was purified by FC (CH₂Cl₂/cyclohexane, 1:1) to afford orange-yellow crystalline powder. Yield: 0.155 g (0.220 mmol, 88%). Mp: 75–77 °C. R_f = 0.73 (CH₂Cl₂/cyclohexane, 1:1). ¹H NMR (200 MHz, CDCl₃): δ 0.87–0.93 (m, 6H), 1.22–1.47 (m, 12H), 1.53–1.63 (m, 4H), 2.82 (t, ³J = 7.2 Hz, 4H), 3.09 (s, 4H), 6.66 (s, 2H), 7.09–7.14

(m, 4H), 7.20–7.26 (m, 4H). ^{13}C NMR (50 MHz, CDCl_3): δ 14.1, 22.5, 28.2, 29.7, 31.3, 36.06, 39.6, 111.3, 127.0, 127.1, 129.0, 129.4, 130.7, 136.3, 136.8. UV/vis (CH_2Cl_2): λ_{max} (ϵ) 265 nm ($22500 \text{ L}\cdot\text{mol}^{-1}\cdot\text{cm}^{-1}$), 333 (12000), 390 sh (3000). MS (ESI⁺): m/z 704 [M]⁺, 727 [M + Na]⁺, 743 [M + K]⁺. MS (ESI⁻): m/z 703 [M - H]⁻. HRMS (ESI⁺): m/z [M]⁺ calcd for $\text{C}_{34}\text{H}_{40}\text{S}_8$ ⁺ 704.08902, found 704.08980. CV (vs SCE, CH_2Cl_2): $E_{1/2}^{\text{ox1}} = 0.58 \text{ V}$, $E_{1/2}^{\text{ox2}} = 0.78 \text{ V}$.

Computational Methods. Initial size and geometry estimations of tetrathiafulvalene and azobenzene building blocks were performed with HyperChem⁴⁵ using the PM3 and HF/3-21G methods. All electronic structure analyses of the isomers of **8** were performed with Gaussian 09 Rev. D.01.⁴⁶ Geometries were optimized with the B3LYP functional and the 6-31G* basis set in the gas phase; the effect of CH_2Cl_2 as solvent was modeled using the polarized continuum model (PCM) employing UAKS radii. UV/vis spectra were obtained from TDDFT calculations with the PBE0 functional and 6-31G* basis set allowing for 40 excited singlet states. In order to locate potential minima the configuration space was sampled at 300 K using Car-Parrinello molecular dynamics (CPMD⁴⁷ program package) with a time step of 4 au and a fictitious orbital mass of 400 au employing the PBE exchange-correlation functional in conjunction with Troullier–Martins normconserving pseudopotentials and a 70 Ry plane wave cutoff.

■ ASSOCIATED CONTENT

● Supporting Information

NMR, MS, and UV/vis spectra, CV experimental details and additional CV plots, and computational details. This material is available free of charge via the Internet at <http://pubs.acs.org>.

■ AUTHOR INFORMATION

Corresponding Authors

*E-mail: vazov@uni-bremen.de.

*E-mail: marcus.boeckmann@uni-muenster.de.

Notes

The authors declare no competing financial interest.

■ ACKNOWLEDGMENTS

We are grateful to Dr. T. Dülcks, Ms. D. Kemken (MS), Dr. Uli Papke (HR-MS, TU Braunschweig), and Dr. J. Warneke (NMR) for their help with the characterization of the new compounds. M.C.B. and N.L.D. acknowledge funding from DFG within TRR 61 and computer time at the University of Münster's high-performance facility.

■ REFERENCES

- (1) Luo, D.-G.; Xue, T.; Yau, K.-W. *Proc. Natl. Acad. Sci. U.S.A.* **2008**, *105*, 9855–9862. (b) Bohran, B.; Souto, M. L.; Imai, H.; Shichida, Y.; Nakanishi, K. *Science* **2000**, *288*, 2209–2212.
- (2) (a) Warshel, A. *Nature* **1976**, *260*, 679–68. (b) Honig, B. *Annu. Rev. Phys. Chem.* **1978**, *29*, 31–57.
- (3) (a) Merino, E. *Chem. Soc. Rev.* **2011**, *40*, 3835–3853. (b) Bandara, H. M. D.; Burdette, S. C. *Chem. Soc. Rev.* **2012**, *41*, 1809–1825.
- (4) *Molecular Switches*; Feringa, B. L., Browne, R. W., Eds.; Wiley-VCH: Weinheim, 2011.
- (5) (a) Merino, E.; Ribagorda, M. *Beilstein J. Org. Chem.* **2012**, *8*, 1071–1090. (b) Russew, M.-M.; Hecht, S. *Adv. Mater.* **2010**, *22*, 3348–3360. (c) Bléger, D.; Liebig, T.; Thiermann, R.; Maskos, M.; Rabe, J. P.; Hecht, S. *Angew. Chem., Int. Ed.* **2011**, *50*, 12559–12563.
- (6) Yagai, S.; Karatsu, T.; Kitamura, A. *Chem.—Eur. J.* **2005**, *11*, 4054–4063.
- (7) Beharry, A. A.; Woolley, G. A. *Chem. Soc. Rev.* **2011**, *40*, 4422–4437.
- (8) (a) Schukat, G.; Fanghänel, E. *Sulfur Rep.* **1996**, *18*, 1–294. (b) Segura, J. L.; Martín, N. *Angew. Chem., Int. Ed.* **2001**, *40*, 1372–1409. (c) Fabre, J. M. *Chem. Rev.* **2004**, *104*, 5133–5150. (d) *TTF Chemistry.*

Fundamentals and Applications of Tetrathiafulvalene; Yamada, J., Sugimoto, T., Eds.; Springer: Heidelberg, 2004.

(9) (a) Wudl, F. *Acc. Chem. Res.* **1984**, *17*, 227–232. (b) Bryce, R. M. *Adv. Mater.* **1999**, *11*, 11–23. (c) Bendikov, M.; Wudl, F.; Perepichka, D. F. *Chem. Rev.* **2004**, *104*, 4891–4945.

(10) Canevet, D.; Sallé, M.; Zhang, G.; Zhang, D.; Zhu, D. *Chem. Commun.* **2009**, 2245–2269.

(11) (a) Bryce, M. R. *J. Mater. Chem.* **2000**, *10*, 589–598. (b) Nielsen, M. B.; Lomholt, C.; Becher, J. *Chem. Soc. Rev.* **2000**, *29*, 153–164. (c) Becher, J.; Jeppesen, J. O.; Nielsen, K. *Synth. Met.* **2003**, *133–134*, 309–315.

(12) (a) Pease, A. R.; Jeppesen, J. O.; Stoddart, J. F.; Luo, Y.; Collier, C. P.; Heath, J. R. *Acc. Chem. Res.* **2001**, *34*, 433–444. (b) Moonen, N. N. P.; Flood, A. H.; Fernández, J. M.; Stoddart, J. F. *Top. Curr. Chem.* **2005**, *262*, 99–132. (c) Klajn, R.; Stoddart, J. F.; Grzybowski, B. A. *Chem. Soc. Rev.* **2010**, *39*, 2203–2237.

(13) (a) Nielsen, K. A.; Cho, W.-S.; Lyskawa, J.; Levillain, E.; Lynch, V. M.; Sessler, J. L.; Jeppesen, J. O. *J. Am. Chem. Soc.* **2006**, *128*, 2444–2451. (b) Nielsen, K. A.; Sarova, G. H.; Martín-Gomis, L.; Fernández-Lázaro, F.; Stein, P. C.; Sanguinet, L.; Levillain, E.; Sessler, J. L.; Guldi, D. M.; Sastre-Santos, Á.; Jeppesen, J. O. *J. Am. Chem. Soc.* **2008**, *130*, 460–462. (c) Nielsen, K. A.; Martín-Gomis, L.; Sarova, G. H.; Sanguinet, L.; Gross, D. E.; Fernández-Lázaro, F.; Stein, P. C.; Levillain, E.; Sessler, J. L.; Guldi, D. M.; Sastre-Santos, Á.; Jeppesen, J. O. *Tetrahedron* **2008**, *64*, 8449–8463. (d) Park, J. S.; Le Derf, F.; Beijer, C. M.; Lynch, V. M.; Sessler, J. L.; Nielsen, K. A.; Johnsen, C.; Jeppesen, J. O. *Chem.—Eur. J.* **2010**, *16*, 848–854.

(14) (a) Düker, M. H.; Schäfer, H.; Zeller, M.; Azov, V. A. *J. Org. Chem.* **2013**, *78*, 4905–4912. (b) Düker, M. H.; Gómez, R.; Vande Velde, C. M. L.; Azov, V. A. *Tetrahedron Lett.* **2011**, *52*, 2881–2884.

(15) (a) Le Derf, F.; Mazari, M.; Mercier, N.; Levillain, E.; Trippé, G.; Riou, A.; Richomme, P.; Becher, J.; Garin, J.; Orduna, J.; Gallego-Planas, N.; Gorgues, A.; Sallé, M. *Chem.—Eur. J.* **2001**, *7*, 447–455. (b) Simonsen, K. B.; Thorup, N.; Becher, J. *Synthesis* **1997**, 1399–1404. (c) Lau, J.; Blanchard, P.; Riou, A.; Jubault, M.; Cava, M. P.; Becher, J. *J. Org. Chem.* **1997**, *62*, 4936–4942. (d) Takimiya, K.; Imamura, K.; Shibata, Y.; Aso, Y.; Ogura, F.; Otsubo, T. *J. Org. Chem.* **1997**, *62*, 5567–5574. (e) Bertho-Thoraval, F.; Robert, A.; Souizi, A.; Boubekeur, K.; Batail, P. *J. Chem. Soc., Chem. Commun.* **1991**, 843–845. (f) Röhrich, J.; Müllen, K. *J. Org. Chem.* **1992**, *57*, 2374–2379.

(16) (a) Goldenberg, L. M.; Bryce, M. R.; Wegener, S.; Petty, M. C.; Cresswell, J. P.; Lednev, I. K.; Hester, R. E.; Moore, J. N. *J. Mater. Chem.* **1997**, *7*, 2033–2037. (b) Sako, K.; Kusakabe, M.; Fujino, H.; Feng, S. X.; Takemura, H.; Shinmyozu, T.; Tatemitsu, H. *Synth. Met.* **2003**, *137*, 899–900. (c) Wen, G.; Zhang, D.; Huang, Y.; Zhao, R.; Zhu, L.; Shuai, Z.; Zhu, D. *J. Org. Chem.* **2007**, *72*, 6247–6250. (d) Wang, C.; Chen, Q.; Sun, F.; Zhang, D.; Zhang, G.; Huang, Y.; Zhao, R.; Zhu, D. *J. Am. Chem. Soc.* **2010**, *132*, 3092–3096.

(17) Castellanos, S.; Grubert, L.; Stöber, R.; Hecht, S. *J. Phys. Chem. C* **2013**, *117*, 23529–23538.

(18) See the Supporting Information for 1D and 2D NMR, MS, and UV/vis spectra, CV experimental details and additional CV plots, and computational details.

(19) (a) Düker, M. H.; Kutter, F.; Dülcks, T.; Azov, V. A. *Supramol. Chem.* **2014**, *26*, 552–560. (b) Abdel-Mottaleb, M. M. S.; Gomar-Nadal, E.; Surin, M.; Uji, H.; Mamdouh, W.; Veciana, J.; Lemaur, V.; Rovira, C.; Cornil, J.; Lazzaroni, R.; Amabilino, D. B.; De Feyter, S.; De Schryver, F. C. *J. Mater. Chem.* **2005**, *15*, 4601–4615.

(20) We use *cis/trans*-notation for tetrathiafulvalene moieties and *Z/E*-notation for azobenzene moieties to avoid confusion concerning their stereochemistry in TTF–AB macrocycles.

(21) (a) Simonsen, K. B.; Svenstrup, N.; Lau, J.; Simonsen, O.; Mork, P.; Kristensen, G. J.; Becher, J. *Synthesis* **1996**, 407–418. (b) Svenstrup, N.; Rasmussen, K. M.; Hansen, T. K.; Becher, J. *Synthesis* **1994**, 809–812.

(22) (a) Joussetme, B.; Blanchard, P.; Gallego-Planas, N.; Delaunay, J.; Allain, M.; Richomme, P.; Levillain, E.; Roncali, J. *J. Am. Chem. Soc.* **2003**, *125*, 2888–2889. (b) Joussetme, B.; Blanchard, P.; Gallego-

Planas, N.; Levillain, E.; Delaunay, J.; Allain, M.; Richomme, P.; Roncali, J. *Chem.—Eur. J.* **2003**, *9*, 5297–5306.

(23) (a) Li, Z. T.; Stein, P. C.; Becher, J.; Jensen, D.; Mark, P.; Svenstrup, N. *Chem.—Eur. J.* **1996**, *2*, 624–633. (b) Le Derf, F.; Mazari, M.; Mercier, N.; Levillain, E.; Trippé, G.; Riou, A.; Richomme, P.; Becher, J.; Garin, J.; Orduna, J.; Gallego-Planas, N.; Gorgues, A.; Sallé, M. *Chem.—Eur. J.* **2001**, *7*, 447–455.

(24) Controlled using ESI–MS.

(25) No individual TTF–AB conjugates could be isolated from the reaction between dithiolates *trans*-/*cis*-3 and *m*-azobenzene (Z)-4.

(26) For examples of locking of azobenzene isomerization by macrocycle formation, see: (a) Yamamura, M.; Okazaki, Y.; Nabeshima, T. *Chem. Commun.* **2012**, *48*, 5724–5726. (b) Yamamura, M.; Yamakawa, K.; Okazaki, Y.; Nabeshima, T. *Chem.—Eur. J.* **2014**, DOI: 10.1002/chem.201404620.

(27) Xu, Y. W.; Smith, M. D.; Krause, J. A.; Shimizu, L. S. *J. Org. Chem.* **2009**, *74*, 4874–4877.

(28) ¹H NMR resonances of the bridging –CH₂– groups appear as slightly broadened singlets for all *cis*-TTF 1 + 1 macrocycles and as doublet of doublets with ²J = 10.8–14.0 Hz for all *trans*-TTF 1 + 1 macrocycles.

(29) Due to the possibility of flipping over the edge of the TTF moiety, aromatic resonances appear as AA'XX' in the ¹H NMR of *cis*-(E)-8. Such flipping is impossible for *trans*-(E)-8, and aromatic resonances appear as four separate doublet of doublets.

(30) For an illustrative example of macrocyclic structures with TTF groups serving as an element of planar chirality, see: Ballardini, R.; Balzani, V.; Becher, J.; Di Fabio, A.; Gandolfi, M. T.; Mattersteig, G.; Nielsen, M. B.; Raymo, F. M.; Rowan, S. J.; Stoddart, J. F.; White, A. J. P.; Williams, D. J. *J. Org. Chem.* **2000**, *65*, 4120–4126.

(31) In rigid azobenzene macrocycles, planar chirality can be imposed by other groups displaying restricted rotation such as naphthalene, but not by AB itself; see, for example: (a) Mathews, M.; Tamaoki, N. *J. Am. Chem. Soc.* **2008**, *130*, 11409–11416. (b) Basheer, M. C.; Oka, Y.; Mathews, M.; Tamaoki, N. *Chem.—Eur. J.* **2010**, *16*, 3489–3496.

(32) Harada, J.; Ogawa, K.; Tomoda, S. *Acta Crystallogr. B* **1997**, *662*–672.

(33) 5,6-Dihydrodibenzo[*c,g*][1,2]diazocine (azobenzenes with a C2-bridge between two *o*-positions) and its derivatives favor (Z)-conformation: (a) Siewertsen, R.; Neumann, H.; Buchheim-Stehn, B.; Herges, R.; Nather, C.; Renth, F.; Temps, F. *J. Am. Chem. Soc.* **2009**, *131*, 15594–15595. (b) Böckmann, M.; Doltsinis, N. L.; Marx, D. *Angew. Chem., Int. Ed.* **2010**, *49*, 3382–3384. (c) Sell, H.; Nather, C.; Herges, R. *Beilstein J. Org. Chem.* **2013**, *9*, 1–7.

(34) For an example of a rigid azobenzenophane with thermodynamically stable (Z)-isomer, see: Norikane, Y.; Katoh, R.; Tamaoki, N. *Chem. Commun.* **2008**, 1898–1900.

(35) For macrocyclic azobenzenes in which the 4- and 4'-positions were connected by a short covalent chain, see: Funke, U.; Grützmacher, H.-F. *Tetrahedron* **1987**, *43*, 3787–3795.

(36) The rate of *cis*-(Z)-8 to *cis*-(E)-8 interconversion is about 2–3 times faster than that of *trans*-(Z)-8 to *trans*-(E)-8, making the characterization of *cis*-(Z)-8 particularly difficult.

(37) Chloroform was deactivated before the NMR measurements using Al₂O₃. Still, according to our previous experience, intrinsic chloroform acidity can lead to *cis*–*trans* isomerization of TTF groups upon prolonged keeping at elevated temperatures.

(38) For an example of photochemical actuation of the electronic properties of π -conjugated systems, see ref 22.

(39) Thus, although *cis*–*trans* isomerization of TTF can be also induced photochemically, we do not designate it as a photochemical switch on Figure 1 since its isomerization does not influence electrochemical properties of the macrocycles.

(40) (a) Gritzner, G.; Kuta, J. *Pure Appl. Chem.* **1984**, *56*, 461–466. (b) Connely, N. G.; Geiger, W. E. *Chem. Rev.* **1996**, *96*, 877–910.

(41) Cardona, C. M.; Li, W.; Kaifer, A. E.; Stockdale, D.; Bazan, G. C. *Adv. Mater.* **2011**, *23*, 2367–2371.

(42) (a) Böckmann, M.; Doltsinis, N. L.; Marx, D. *J. Chem. Phys.* **2012**, *137*, 22A505. (b) Böckmann, M.; Braun, S.; Doltsinis, N. L.; Marx, D. J.

Chem. Phys. **2013**, *139*, 084108. (c) Turanský, R.; Konopka, M.; Doltsinis, N. L.; Štich, I.; Marx, D. *ChemPhysChem* **2010**, *11*, 345–348. (d) Turanský, R.; Konopka, M.; Doltsinis, N. L.; Štich, I.; Marx, D. *Phys. Chem. Chem. Phys.* **2010**, *12*, 13922–13932. (e) Konopka, M.; Turanský, R.; Doltsinis, N. L.; Marx, D.; Štich, I. *Adv. Solid State Phys.* **2009**, *48*, 219–235. (f) Böckmann, M.; Doltsinis, N. L.; Marx, D. *J. Phys. Chem. A* **2010**, *114*, 745–754.

(43) (a) Pancur, T.; Renth, F.; Temps, F.; Harbaum, B.; Krüger, A.; Herges, R.; Nather, C. *Phys. Chem. Chem. Phys.* **2005**, *7*, 1985–1989. (b) Siewertsen, R.; Schönborn, J. B.; Hartke, B.; Renth, F.; Temps, F. *Phys. Chem. Chem. Phys.* **2011**, *13*, 1054–1063. (c) Nonnenberg, C.; Gaub, H.; Frank, I. *ChemPhysChem* **2006**, *7*, 1455–1461. (d) Harada, J.; Ogawa, K. *J. Am. Chem. Soc.* **2001**, *123*, 10884–10888. (e) Harada, J.; Ogawa, K. *J. Am. Chem. Soc.* **2004**, *126*, 3539–3544. (f) Harada, J.; Ogawa, K. *Chem. Soc. Rev.* **2009**, *38*, 2244–2252.

(44) Bléger, D.; Schwarz, J.; Brouwer, A. M.; Hecht, S. *J. Am. Chem. Soc.* **2012**, *134*, 20597–20600.

(45) Hyper Chem v. 8.0.6 for Windows, Hypercube Inc.

(46) Gaussian 09, Revision D.01: Frisch, M. J.; Trucks, G. W.; Schlegel, H. B.; Scuseria, G. E.; Robb, M. A.; Cheeseman, J. R.; Scalmani, G.; Barone, V.; Mennucci, B.; Petersson, G. A.; Nakatsuji, H.; Caricato, M.; Li, X.; Hratchian, H. P.; Izmaylov, A. F.; Bloino, J.; Zheng, G.; Sonnenberg, J. L.; Hada, M.; Ehara, M.; Toyota, K.; Fukuda, R.; Hasegawa, J.; Ishida, M.; Nakajima, T.; Honda, Y.; Kitao, O.; Nakai, H.; Vreven, T.; Montgomery, J. A., Jr.; Peralta, J. E.; Ogliaro, F.; Bearpark, M.; Heyd, J. J.; Brothers, E.; Kudin, K. N.; Staroverov, V. N.; Kobayashi, R.; Normand, J.; Raghavachari, K.; Rendell, A.; Burant, J. C.; Iyengar, S. S.; Tomasi, J.; Cossi, M.; Rega, N.; Millam, M. J.; Klene, M.; Knox, J. E.; Cross, J. B.; Bakken, V.; Adamo, C.; Jaramillo, J.; Gomperts, R.; Stratmann, R. E.; Yazyev, O.; Austin, A. J.; Cammi, R.; Pomelli, C.; Ochterski, J. W.; Martin, R. L.; Morokuma, K.; Zakrzewski, V. G.; Voth, G. A.; Salvador, P.; Dannenberg, J. J.; Dapprich, S.; Daniels, A. D.; Farkas, Ö.; Foresman, J. B.; Ortiz, J. V.; Cioslowski, J.; Fox, D. J. Gaussian, Inc., Wallingford, CT, 2009.

(47) Hutter, J. et al. Car-Parrinello Molecular Dynamics: An Ab Initio Electronic Structure and Molecular Dynamics Program; see www.cpm.d.org.